Regulation of ATM/p53-dependent suppression of myc-induced lymphomas by Wip1 phosphatase

Sathyavageeswaran Shreeram,[1] Weng Kee Hee,[1] Oleg N. Demidov,[1] Calvina Kek,[1] Hiroshi Yamaguchi,[2] Albert J. Fornace Jr.,[3] Carl W. Anderson,[4] Ettore Appella,[2] and Dmitry V. Bulavin[1]

[1]Institute of Molecular and Cell Biology, Singapore, 138673
[2]Laboratory of Cell Biology, Center for Cancer Research, National Cancer Institute (NCI), National Institutes of Health (NIH), Bethesda, MD 20892
[3]Department of Genetics and Complex Diseases, Harvard School Of Public Health, Boston, MA 02115
[4]Biology Department, Brookhaven National Laboratory, Upton, NY 11973

The ataxia telangiectasia mutated (ATM) kinase is a key tumor suppressor that regulates numerous cell cycle checkpoints as well as apoptosis. Here, we report that ATM is a critical player in the regulation of apoptosis and lymphomagenesis in the presence of c-myc. In turn, deletion of the inhibitory ATM phosphatase, Wip1, results in ATM up-regulation and suppression of Eμ-myc–induced B cell lymphomas. Using mouse genetic crosses, we show that the onset of myc-induced lymphomas is dramatically delayed in Wip1-null mice in an ATM- and p53-, but not p38 MAPK– or Arf-, dependent manner. We propose that Wip1 phosphatase is critical for regulating the ATM-mediated tumor surveillance network.

CORRESPONDENCE
D.V. Bulavin:
dvbulavin@imcb.a-star.edu.sg

The ataxia telangiectasia mutated (ATM) kinase is involved in transducing signals that are implicated in the regulation of cell cycle checkpoints, apoptosis, and DNA repair (1). The ATM-dependent pathway is activated early in the course of human tumorigenesis and serves as an anticancer barrier that helps to delay or prevent cancer (2). In turn, a deficiency of ATM results in early onset of lymphomas in mice (3), whereas germline mutations in the ATM gene cause ataxia-telangiectasia, a multisystem disorder that is associated with a predisposition to lymphoma and acute leukemia (4). Regulation of the ATM-dependent pathway is complex and involves numerous positive and negative regulators (1). Among the latter, emerging data support a role for ATM phosphatases PP2A and Wip1 in controlling the magnitude and duration of ATM phosphorylation and activity after stress (5, 6).

There is increasing evidence that Wip1 phosphatase can function as an oncogene (7, 8). The Wip1 gene, *PPM1D*, is amplified in ~15% of primary human breast cancers, which leads to Wip1 overexpression. Transformation experiments with rodent fibroblasts have shown that the introduction of Wip1 along with Ras, Myc, or ErbB2 results in enhanced colony formation in soft agar (7, 8). A combination of genetic and molecular studies have established that the oncogenic properties of Wip1 may result from its suppression of p53 functions (7, 8). Along this line, almost all Wip1-overexpressing breast tumors were found to have a structurally intact p53 gene, confirming that Wip1 could functionally inactivate p53 (7).

Regulation of several signaling pathways has been proposed by Wip1 phosphatase. Modulation of the p38 MAPK signaling cascade was shown both in vitro and in vivo (9, 10). We found that activation of p38 MAPK could be critical in rendering Wip1-deficient mice resistant to mammary gland tumors driven by *ErbB2* and Ras oncogenes (10). Further studies, however, revealed that in addition to p38 MAPK (11), Wip1 could efficiently dephosphorylate in vitro the serine residues on p53, H2AX, and Chk2 (6, 12, 13). Likewise, Wip1 phosphatase plays an important role in dephosphorylating ATM both in vitro and in vivo (6).

RESULTS AND DISCUSSION

Activation of the ATM-dependent tumor suppressor network could be critical in the

The online version of this article contains supplemental material.

previously identified resistance of Wip1-deficient mice to tumorigenesis (6, 10). Wip1 phosphatase dephosphorylates ATM at Ser1981 and is required to reset ATM phosphorylation after DNA damage (6). ATM autophosphorylation as well as its binding with the Mre11/Rad50/NBS1 complex are the two major means of ATM activation after DNA damage (1). In turn, ATM autophosphorylation (apparently at several phospho sites; references 14 and 15) is sufficient to fully activate ATM (14). As Wip1 deficiency resulted in up-regulation of ATM activity (6), which could not be fully explained by changes in Ser1981 phosphorylation (5,16), we asked whether Wip1 could dephosphorylate other autophosphorylation sites on ATM. Using an in vitro phosphatase assay, we found that Ser367, but not Ser1893, was efficiently dephosphorylated by Wip1 in vitro (Table I). We further showed that Wip1 directly binds ATM's N terminus (amino acids 1–989) and FAT domain (amino acids 1916–2644; Fig. 1 A), which contain Ser367 and Ser1981, respectively. These data further support a direct role of Wip1 in regulating ATM through dephosphorylation of multiple residues.

To further validate the significance of our findings on the role of Wip1 in regulation of ATM signaling, we identified Wip1-deficient splenocytes as a cell type with a high level of ATM phosphorylation at Ser1987 (human Ser1981). As the spleen is primarily comprised of B cells, we crossed Wip1-deficient mice with Eμ-myc transgenic mice in which the expression of myc is restricted to B lymphocytes (17) to provide a physiologically relevant model for understanding the significance of ATM activation in suppressing tumorigenesis in Wip1-deficient mice. Analysis of splenocytes obtained from $Wip1^{+/+}$ and $Wip1^{-/-}$ mice expressing Eμ-myc revealed increased phosphorylation of ATM, p53 at the ATM target site Ser18 (human Ser15; $Wip1^{+/+}$ Eμ-myc splenocytes showed either no [Fig. 1 B, lane 1] or slight [Fig. 1 B, lane 2] p53 phosphorylation), as well as increased phosphorylation of p38 and its target, HSP-27 (Fig. 1 B and Fig. S1, which is available at http://www.jem.org/cgi/content/full/jem.20061563/DC1). No difference in the phosphorylation of Chk1 Ser345 was observed in splenocytes obtained from $Wip1^{+/+}$ or $Wip1^{-/-}$ mice (Fig. 1 B).

To investigate tumor onset, we used only littermates from the same parents for all of our crosses. Next, we investigated whether ablation of Wip1 protects mice from Eμ-myc–induced B lymphomas. We crossed Wip1-null mice with Eμ-myc transgenic mice and found that $Wip1^{+/-}$ and $Wip1^{-/-}$ mice were considerably more resistant to tumor formation induced by myc than wild-type mice (Fig. 1 C). The median

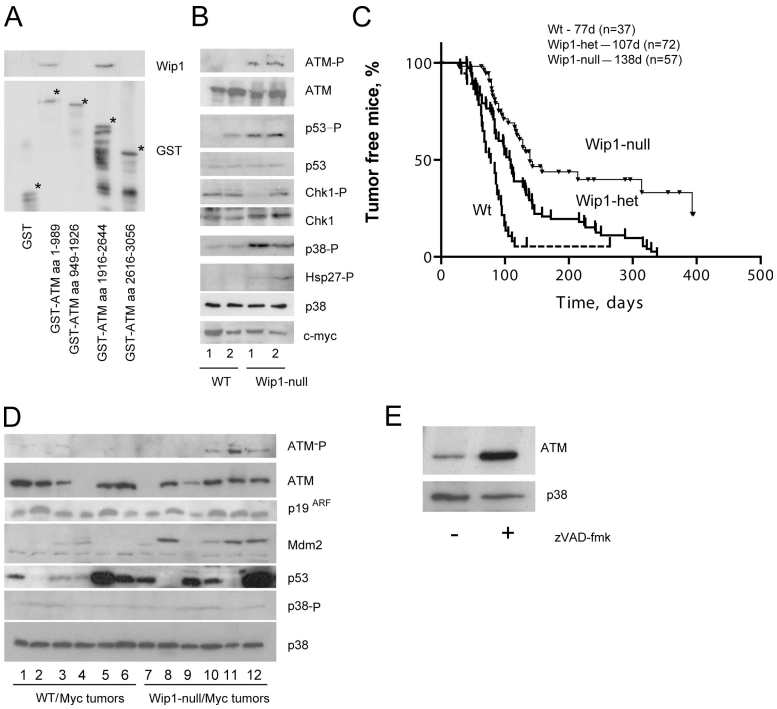

Figure 1. Wip1 deficiency suppressed myc-induced lymphomagenesis. (A) In vitro association of ATM fragments with Wip1. Bacteria-expressed purified His-Wip1 was incubated with purified glutathione *S*-transferase (GST) or different GST-ATM fragments. Wip1 bound to ATM was detected after pull-down with glutathione-sepharose. The appropriate GST fragments are marked with asterisks. (B) Levels of phosphorylation and the expression of different proteins were analyzed in splenocytes from two separate $Wip1^{+/+}$ Eμ-myc and $Wip1^{-/-}$ Eμ-myc mice. (C) The occurrence of lymphomas in $Wip1^{+/+}$, $Wip1^{+/-}$, and $Wip1^{-/-}$ mice bearing the Eμ-myc transgene was analyzed over 400 d. The MLS for different genotypes is shown at the top. (D) The levels of expression of different proteins were analyzed in tumor samples obtained from $Wip1^{+/+}$ Eμ-myc (1–6) or $Wip1^{-/-}$ Eμ-myc (7–12) mice. (E) The level of ATM was analyzed in cultured lymphoma cells with or without caspase inhibitor zVAD-fmk.

Table I. Kinetic parameters for the dephosphorylation of phosphopeptides by rWip1 at pH 7.5, 30°C

Substrate	Sequence	K_m (μM)	k_{cat} (s^{-1})	k_{cat}/K_m ($10^3 \times M^{-1}\ s^{-1}$)
ATM(1981pS)	AFEEGpSQSTTI	31 ± 2	2.9 ± 0.1	94
ATM(367pS)	RSLEIpSQSYTT	38 ± 2	1.5 ± 0.03	39
ATM(1893pS)	NLDSEpSEHFFR	>200	ND[a]	ND[a]
p38(180pT 182pY)	TDDEMpTGpYVAT	31 ± 3	2.0 ± 0.1	64

Values represent averages from three to four independent experiments.
[a]The K_m and k_{cat} values could not be determined due to the high K_m.

lifespan (MLS) in our cohort of $Wip1^{+/+}$ mice was around 77 d. In contrast, the MLS for $Wip1^{+/-}$ mice was 107 d ($P = 0.002$) and for $Wip1^{-/-}$ mice was 138 d ($P < 0.001$).

The appearance of tumors in the Eμ-myc mouse B lymphoma model is due primarily to the high selective pressure placed on the ARF-p53 signaling cascade (18, 19). To understand the spectrum of molecular changes in our set of tumors, we next analyzed extracts for the expression of different proteins. We found that the level of $p19^{Arf}$ was increased in 6 of the 12 analyzed tumors (Fig. 1 D). These tumors also showed either loss (samples 2, 8, and 11) or mutation (samples 5 and 12), confirmed by the sequencing of the cDNAs of p53. We also observed the overexpression of Mdm2 protein in multiple samples (Fig. 1 D). Our data are in agreement with a previous observation showing that high $p19^{Arf}$ levels result from absence of the p53-induced negative feedback loop due to overexpression of Mdm2 or inactivation of p53 (20). Interestingly, analysis of ATM levels revealed a reduction of ATM expression or its loss in multiple wild-type and Wip1-null tumors (15 out of 34 analyzed tumors; Fig. 1 D and not depicted). Importantly, we found that tumors with reduced levels of ATM showed a strong correlation with normal levels of $p19^{Arf}$ and structurally intact p53, supporting the idea that loss of ATM relieves pressure for the inactivation of p53 downstream of myc (Fig. 1 D).

To gain insight into potential mechanisms of ATM loss in Eμ-myc tumors, we checked ATM mRNA by real-time PCR and for the presence of mutations by genomic sequencing. We found no difference in the levels of ATM mRNA between tumor samples that did or did not express ATM; likewise, no mutations in the ATM sequence were found (not depicted). Previous data suggest that ATM can undergo a caspase-dependent degradation upon induction of apoptosis (21, 22). To check this possibility, we treated the cultured lymphoma cells containing reduced levels of ATM with 10 μM of the caspase inhibitor zVAD-fmk (overnight incubation). As shown in Fig. 1 E, inactivation of caspases resulted in a dramatic increase in ATM levels.

We previously reported that activation of p38 MAPK was important in suppressing the early development of mammary gland tumors in Wip1-null mice (10). As it is critical to understand any contribution of increased p38 MAPK signaling to the resistance of Wip1-null mice for Eμ-myc–induced B cell lymphomas, we crossed Wip1-null mice with p38α knock-in mice. In these mice, the p38α regulatory sites Thr180 and Tyr182 are replaced by alanine and phenylalanine, respectively, thus disabling p38α activation by any stimuli (unpublished data). Next, we asked whether the presence of one mutant allele for p38α, which has dominant-negative features, would be sufficient to attenuate p38 activation in Wip1-deficient cells. Deficiency of Wip1 caused an increase in the phosphorylation of HSP27, a downstream target in the p38 MAPK cascade, in unirradiated cells, and mutation of one allele of p38α was sufficient to reduce HSP27 phosphorylation to levels below those found in wild-type dermal fibroblasts (Fig. 2 A, middle, lanes 1, 5, and 9, and Fig. S1). However, despite the fact that p38 MAPK was up-regulated in Wip1-deficient splenocytes expressing Eμ-myc (Fig. 1 B), lowering the level of p38 activation (as in the $p38\alpha^{KI/+}$ mice) had no apparent effect on the onset of B cell lymphomas (Fig. 2 B) because $Wip1^{-/-}p38\alpha^{KI/+}$ Eμ-myc mice remained tumor resistant (MLS = 131 d for

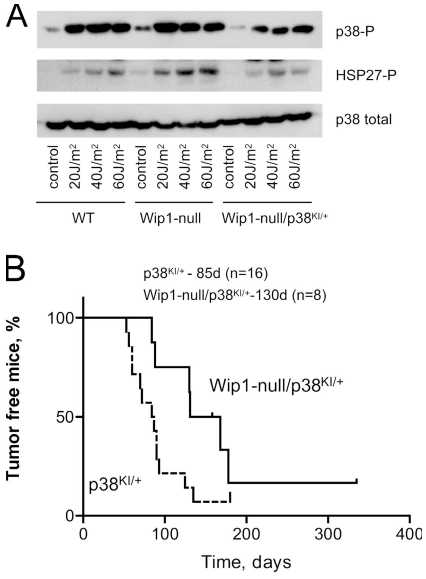

Figure 2. p38 MAPK is not required to render Wip1-deficient mice resistant to Myc-induced lymphomas. (A) The levels of phosphorylation of p38 and its target HSP27 were analyzed in dermal fibroblasts purified from wild-type, $Wip1^{-/-}$, or $Wip1^{-/-}$ $p38\alpha^{Ki/+}$ mice. Cells were treated with different doses of ultraviolet C and harvested 1 h later. (B) The occurrence of lymphomas in $Wip1^{+/+}$ $p38\alpha^{Ki/+}$ or $Wip1^{-/-}$ $p38\alpha^{Ki/+}$ mice bearing the Eμ-myc transgene was analyzed, and the MLS for the different genotypes is shown at the top.

$Wip1^{-/-}p38\alpha^{KI/+}$ Eμ-myc vs. 85 d for $p38\alpha^{KI/+}$ Eμ-myc mice; $P = 0.038$).

Development of lymphomas in the Eμ-myc model is dependent on the suppression of Arf/p53 signaling, as deletion of only one copy of either gene is sufficient to dramatically accelerate tumor onset (18, 19). In turn, Wip1-deficient cells possess a high level of p53 activity (10) and phosphorylation at Ser18 (Fig. 1 B). To understand whether inactivation of *Trp53* or $p19^{Arf}$ is sufficient to eliminate the difference between $Wip1^{+/+}$ Eμ-myc and $Wip1^{-/-}$ Eμ-myc mice, we crossed $Wip1^{+/-}$ Eμ-myc mice with either $Wip1^{+/-}p53^{+/-}$ or $Wip1^{+/-}Arf^{+/-}$ mice. No difference in tumor appearance between $Wip1^{+/+}p53^{+/-}$ Eμ-myc and $Wip1^{-/-}p53^{+/-}$ Eμ-myc mice was found ($P = 0.43$); both groups of mice rapidly succumbed to tumors within 45 d of birth (Fig. 3 A). Analysis of the p53 status revealed loss of the second p53 allele in tumors that developed in 60% (6 out of 10) of $Wip1^{+/+}$ Eμ-myc and 50% (6 out of 12) of $Wip1^{-/-}$ Eμ-myc mice. In contrast, although all $Wip1^{+/+}Arf^{+/-}$ Eμ-myc mice rapidly developed tumors (Fig. 3 B) with a time of onset that was not significantly different from those in $Wip1^{+/+}p53^{+/-}$ Eμ-myc mice (Fig. 3 A), $Wip1^{-/-}Arf^{+/-}$ Eμ-myc mice remained tumor resistant ($P < 0.001$).

Next, we intercrossed $Arf^{+/-}Wip1^{-/-}$ Eμ-myc mice to check whether the loss of both copies of *Arf* would accelerate the onset of lymphomas in a Wip1-deficient background. We found that, in the absence of both copies of *Arf*, Wip1-deficient mice remained tumor resistant. In a group of 10 mice, all survived beyond 80 d without any sign of tumors.

As the ATM kinase appeared to be activated in Wip1-null splenocytes, resulting in increased p53 phosphorylation at Ser18 (Fig. 1 B), we next checked the contribution of ATM in suppressing tumorigenesis induced by myc. Analysis of lymphoma formation revealed that heterozygocity of ATM did not accelerate tumorigenesis in either $Wip1^{+/+}$ Eμ-myc or $Wip1^{-/-}ATM^{+/-}$ Eμ-myc mice. Analysis of tumors that arose in the $ATM^{+/-}$ Eμ-myc mice showed that none of 12 tumors lost the second ATM allele. Next, we analyzed tumor onset in an ATM-null background. As ATM-null mice are prone to development of T cell, but not B cell, lymphomas (3), all tumors in the $ATM^{-/-}$ Eμ-myc background were analyzed and found to be B cell–derived lymphomas ($B220^+$ $CD4^-$; not depicted). Importantly, tumor onset for $Wip1^{-/-}ATM^{-/-}$ Eμ-myc mice (Fig. 3 C) was significantly accelerated compared with $Wip1^{-/-}$ Eμ-myc mice (69 vs. 138 d [Fig. 1 C]; $P < 0.001$); thus, suppression of Eμ-myc–induced lymphomagenesis in Wip1-deficient mice is dependent on p53 (Fig. 3 A) and ATM (Fig. 3 C).

As tumor development in Eμ-myc lymphomas is due primarily to changes in rates of cell proliferation or apoptosis, we next checked the proliferation and apoptotic rates of tumors arising in different genetic backgrounds. Although no difference in the rates of proliferation was found between different genotypes (Fig. 4 A), the level of $TUNEL^+$ cells (an apoptosis marker) was reduced in mice with an $ATM^{-/-}$ background to the levels observed for either $p53^{+/-}$ or

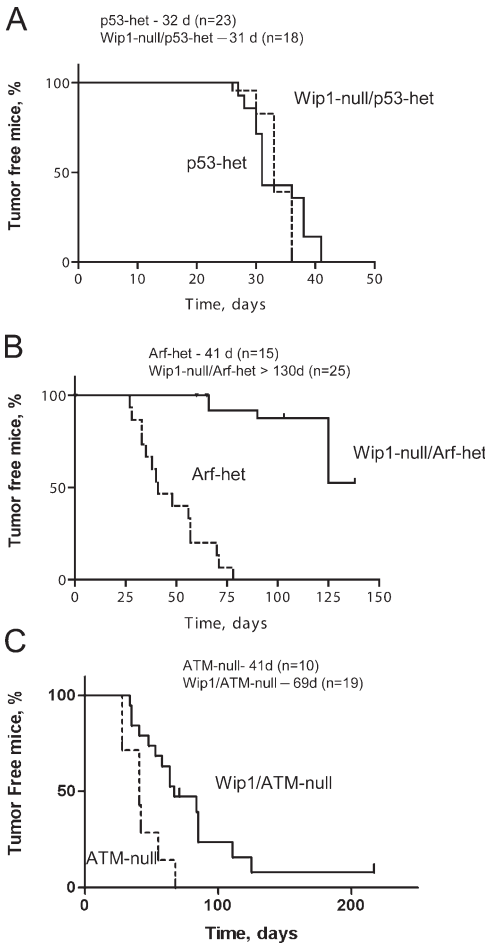

Figure 3. Wip1 deficiency suppressed myc-induced lymphomagenesis in an ATM/p53-dependent, Arf-independent manner. (A) The occurrence of lymphomas in $Wip1^{+/+}$ $p53^{+/-}$ or $Wip1^{-/-}$ $p53^{+/-}$ mice bearing the Eμ-myc transgene was analyzed, and the MLS for different genotypes is shown at the top. (B) The occurrence of lymphomas in $Wip1^{+/+}$ $Arf^{+/-}$ and $Wip1^{-/-}$ $Arf^{+/-}$ mice bearing the Eμ-myc transgene was analyzed, and the MLS for different genotypes is shown at the top. (C) The occurrence of lymphomas in $Wip1^{+/+}$ $ATM^{-/-}$ and $Wip1^{-/-}$ $ATM^{-/-}$ mice bearing the Eμ-myc transgene was analyzed, and the MLS for different genotypes is shown at the top.

$Arf^{+/-}$ tumors (Fig. 4 B). Interestingly, loss of one copy of *Arf* almost completely eliminated apoptosis in $Wip1^{+/+}$/$Arf^{+/-}$ Eμ-myc tumors, whereas $Wip1^{-/-}$/$Arf^{+/-}$ Eμ-myc tumors retained levels of apoptosis comparable to those of wild-type/Eμ-myc tumors.

We next investigated whether the $p19^{Arf}$–Mdm2–p53 pathway had been inactivated in the Eμ-myc tumors arising in ATM mutant mice, as inactivation is common in wild-type and Wip1-deficient backgrounds (Fig. 1 D). The level of $p19^{Arf}$ is a sensitive indicator for the functionality of this pathway (20). Although ~40% of tumors arising in wild-type and Wip1-deficient mice overexpressed Arf (Fig. 1 D), which is similar to the incidence reported by others (18–20), none of the tumors from $Wip1^{+/+}$/$ATM^{-/-}$ mice (0 of 12, with

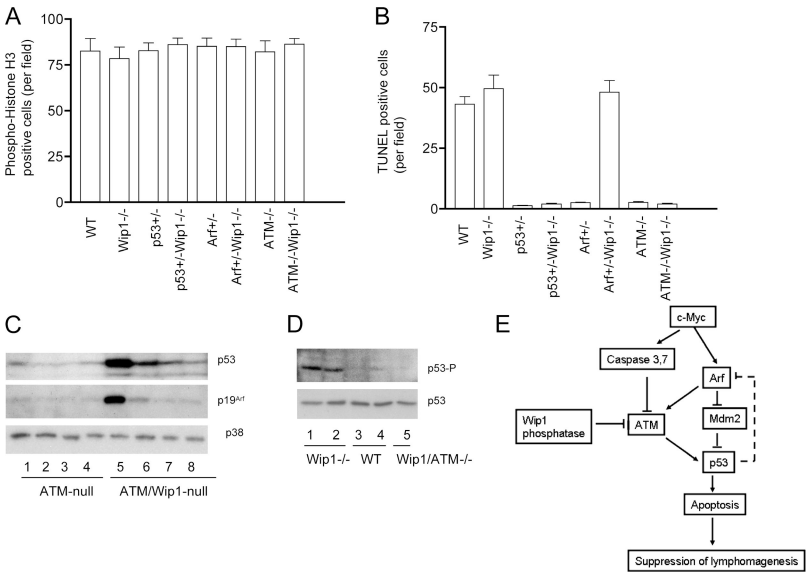

Figure 4. ATM is critical in the activation of myc-induced apoptosis. (A) The mitotic index based on analysis of phospho-histone H3$^+$ cells was determined in tumors that arose in different backgrounds. (B) Apoptosis based on analysis of TUNEL$^+$ cells was measured in tumors that arose in different backgrounds. (C) The levels of p53, p19^{Arf}, and p38 (loading control) were analyzed in ATM$^{-/-}$ Eμ-myc tumors with wild-type (1–4) or Wip1$^{-/-}$ (5–8) backgrounds. (D) The levels of p53 and p53 phosphorylation at Ser18 were analyzed in wild-type, Wip1, and Wip1/ATM double-deficient splenocytes expressing Eμ-myc. (E) A diagram illustrating the role of the Wip1 phosphatase in suppressing lymphomagenesis in the presence of myc.

4 shown in Fig. 4 C, lanes 1–4) did so. Moreover, none of the tumors from Wip1$^{+/+}$/ATM$^{-/-}$ mice showed loss or mutation of p53 (0 of 12, with 4 shown in Fig. 4 C, lanes 1–4).

Removal of ATM accelerated tumor onset in Wip1-deficeint mice (Fig. 3 C); however, analysis of the p19^{Arf}–p53 pathway revealed its deregulation in 2 of the 12 analyzed tumors that developed in Wip1/ATM double-deficient mice expressing Eμ-myc (1 shown in Fig. 4 C, lane 5). Both tumors showed a high level of p53 and p19^{Arf}, and subsequent sequencing revealed mutations in the p53 cDNAs (gaa [Glu] to aaa [Lys] at codon 283, and gcc [Ala] to gac [Asp] at codon 158). Thus, besides ATM, Wip1-deficient cells may use additional pathway(s) to activate p53.

Recent data suggest that Wip1 directly dephosphorylates Ser15 of human p53 (12). As p53 Ser15 is a direct target for the ATM kinase, which, in turn, is activated in Wip1-deficient cells, we next asked whether removal of ATM would be sufficient to reduce the level of p53 phosphorylation at Ser18 (human Ser15). Analysis of p53 Ser18 phosphorylation, as shown in Fig. 4 D, revealed that deletion of ATM completely eliminated the difference between wild-type and Wip1-null splenocytes. Thus, although additional mechanisms besides ATM may contribute to p53 activation in Wip1-deficient B cells, they are independent of p53 phosphorylation at Ser15 and Chk1 at Ser345 (Figs. 1 B and 4 D).

Here, we show that deficiency of Wip1 phosphatase contributes to suppression of myc-induced lymphomagenesis in an ATM/p53-dependent manner. In turn, the role of ATM in suppressing the early onset of lymphomas is critical, as deletion of ATM from Eμ-myc mice dramatically accelerated tumorigenesis (MLS = 77 d for ATM$^{+/+}$ Eμ-myc vs. 41 d for ATM$^{-/-}$ Eμ-myc mice), and some Eμ-myc tumors showed a loss or a reduction in ATM expression. Loss of ATM resulted in a dramatic decrease in the rate of apoptosis and removed the strong selective pressure for functional inactivation of the p53 apoptotic pathway during myc-induced lymphomagenesis (Fig. 4, B and C). Importantly, ATM could be critical during physiological class switching for preventing myc-induced tumorigenesis by inhibiting translocations between c-myc and the IgH locus in primary B cells (23).

Myc is a potent inducer of apoptosis, and reduction or loss of ATM protein in Eμ-myc–induced lymphomas appeared to be through its caspase-dependent degradation (Fig. 1 E). As the presence of ATM is critical in executing the p53 apoptotic pathway during myc-induced lymphomagenesis (Fig. 4 B), it is possible that in the course of tumorigenesis a substantial number of B cells have reduced ATM levels due to myc-dependent activation of caspases. In turn, when the level of ATM falls below the threshold required to maintain activation of the p53 apoptotic pathway, development of lymphomas occurs. However, even in those cases when the level of ATM is lowered to reduce apoptosis and cause lymphoma development in wild-type mice, deficiency in Wip1 phosphatase will activate the remaining pool of ATM (Fig. 4 E; reference 6). This activation, in turn, signals to p53, which initiates apoptosis at a level sufficient to protect B cells from myc-induced lymphomagenesis, even when both copies of p19^{Arf} have been lost.

It was well established that protection from tumorigenesis in the Eμ-myc model of B lymphomas is dependent on the presence of p53 and Arf, as deletion of only one copy of either gene is sufficient to dramatically accelerate tumor onset (18, 19). In turn, a recent analysis of the effects of Arf revealed that its overexpression is sufficient to increase ATM-dependent signaling to p53, probably through a Tip60-dependent acetylation of ATM (24, 25). In a similar scenario, overexpression of E2F1, another efficient inducer of Arf expression, was shown to result in the phosphorylation of p53 at serine 15 via ATM (26). Thus, activation of p53 in the presence of myc can be achieved through both the ATM signaling network as well as through Arf-mediated inhibition of Mdm2-dependent repression and degradation of p53 (Fig. 4 E). On the other hand, overexpression of Wip1, as occurs in certain types of cancers (7, 8), may accelerate tumorigenesis by inhibiting ATM. In turn, inactivation of the Wip1 phosphatase with subsequent activation of ATM/p53 signaling could be critical for suppressing tumorigenesis in B cells and likely other tumor types.

MATERIALS AND METHODS

Mouse strains. All animal protocols used in this study were approved by the Institute of Molecular and Cell Biology Animal Safety and Use Committee. We crossed Wip1$^{+/-}$ mice with p53$^{+/-}$, p19$^{Arf+/-}$, ATM$^{+/-}$, p38α$^{KI/+}$ (unpublished data), or FVB/N Eμ-myc mice to obtain mice of different genotypes. p19^{Arf} heterozygous and ATM heterozygous mice were obtained from the NCI Mouse Repository and The Jackson Laboratory, respectively. FVB/N Eμ-myc mice were from Charles River Laboratories (Wilmington, MA). Mice were checked for tumors twice a week by palpation.

Western blotting. We prepared cell lysates as described previously (10). Immunoblots were probed with antibodies to phospho-ATM (Ser 1981; Chemicon International), phospho-p53 (Ser15), phospho-p38 (Thr180/Tyr182), phospho-HSP27 (Ser82), and total p38 (C-20; Santa Cruz Biotechnology, Inc.). Antibody to ATM (2C1) was from GeneTex and antibody to p19^{Arf} was from Abcam. As secondary antibodies, we used peroxidase-conjugated IgGs (Jackson ImmunoResearch Laboratories), followed by enhanced chemiluminescence detection (GE Healthcare).

Real-Time PCR. Total RNA was extracted using Trizol reagent according to the manufacturer's protocol (Invitrogen). cDNA synthesis was performed using a mixture of random and oligo(dT) primers and SuperScript II reverse transcriptase (Invitrogen). Real-time PCR analysis of the mouse ATM, Cdkn2a, and the reference mRNA for cyclophilin A was performed with the LightCycler Rapid Thermal Cycler System (Roche Diagnostics Ltd.). Reactions were performed in a 10-μl volume with 1 μM primers, nucleotides, and LightCycler-DNA Master SYBR Green I mix (Roche Diagnostics Ltd.). A typical protocol included a 10-min denaturation step followed by 40 cycles with a 95°C denaturation for 20 s, 59°C annealing for 20 s, and 72°C extension for 20 s. For quantitative analysis of the p19^{Arf} genomic locus, we purified genomic DNA using the DNeasy Tissue kit (QIAGEN) and analyzed four different genomic fragments spanning 18 kb of the p19^{Arf} genomic locus using the above protocol. The primer sequences are available upon request.

Online supplemental material. Fig. S1 shows quantitative analysis of the results in Figs. 1 B and 2A. It is available at http://www.jem.org/cgi/content/full/jem.20061563/DC1.

This work was supported by the Agency for Science, Technology and Research (Singapore). C.W. Anderson was supported in part by a grant from the US Department of Energy. The research for H. Yamaguchi and E. Appella was supported by the Intramural Research Program of the NIH.

The authors have no conflicting financial interests.

Submitted: 25 July 2006
Accepted: 17 November 2006

REFERENCES

1. Kastan, M.B., and J. Bartek. 2004. Cell-cycle checkpoints and cancer. *Nature*. 432:316–323.
2. Bartkova, J., Z. Horejsi, K. Koed, A. Kramer, F. Tort, K. Zieger, P. Guldberg, M. Sehested, J.M. Nesland, C. Lukas, et al. 2005. DNA damage response as a candidate anti-cancer barrier in early human tumorigenesis. *Nature*. 434:864–870.
3. Barlow, C., S. Hirotsune, R. Paylor, M. Liyanage, M. Eckhaus, F. Collins, Y. Shiloh, J.N. Crawley, T. Ried, D. Tagle, and A. Wynshaw-Boris. 1996. Atm-deficient mice: a paradigm of ataxia telangiectasia. *Cell*. 86:159–171.
4. Shiloh, Y., and M.B. Kastan. 2001. ATM: genome stability, neuronal development, and cancer cross paths. *Adv. Cancer Res*. 83:209–254.
5. Goodarzi, A.A., J.C. Jonnalagadda, P. Douglas, D. Young, R. Ye, G.B. Moorhead, S.P. Lees-Miller, and K.K. Khanna. 2004. Autophosphorylation of ataxia-telangiectasia mutated is regulated by protein phosphatase 2A. *EMBO J*. 23:4451–4461.
6. Shreeram, S., O.N. Demidov, W.K. Hee, H. Yamaguchi, N. Onishi, C. Kek, O.N. Timofeev, C. Dungeon, A.J. Fornace, C.W. Anderson, et al. 2006. Wip1 phosphatase modulates ATM-dependent signaling pathways. *Mol. Cell*. 23:757–764.
7. Bulavin, D.V., O.N. Demidov, S. Saito, P. Kauraniemi, C. Phillips, S.A. Amundson, C. Ambrosino, G. Sauter, A.R. Nebreda, C.W. Anderson, et al. 2002. Amplification of *PPM1D* in human tumors abrogates p53 tumor-suppressor activity. *Nat. Genet*. 31:210–215.
8. Li, J., Y. Yang, Y. Peng, R.J. Austin, W.G. van Eyndhoven, K.C.Q. Nguyen, T. Gabriele, M.E. McCurrach, J.R. Marks, T. Hoey, et al. 2002. Oncogenic properties of *PPM1D* located within a breast cancer amplification epicenter at 17q23. *Nat. Genet*. 31:133–134.
9. Takekawa, M., M. Adachi, A. Nakahata, I. Nakayama, F. Itoh, H. Tsukuda, Y. Taya, and K. Imai. 2000. p53-inducible Wip1 phosphatase mediates a negative feedback regulation of p38 MAPK-p53 signaling in response to UV radiation. *EMBO J*. 19:6517–6526.
10. Bulavin, D.V., C. Phillips, B. Nannenga, O. Timofeev, L.A. Donehower, C.W. Anderson, E. Appella, and A.J. Fornace Jr. 2004. Inactivation of the Wip1 phosphatase inhibits mammary tumorigenesis through p38 MAPK-mediated activation of the p16^{Ink4a}-p19^{Arf} pathway. *Nat. Genet*. 36:343–350.
11. Yamaguchi, H., G. Minopoli, O.N. Demidov, D.K. Chatterjee, C.W. Anderson, S.R. Durell, and E. Appella. 2005. Substrate specificity of the human protein phosphatase 2Cδ, Wip1. *Biochemistry*. 44:5285–5294.
12. Lu, X., B. Nannenga, and L.A. Donehower. 2005. PPM1D dephosphorylates Chk1 and p53 and abrogates cell cycle checkpoints. *Genes Dev*. 19:1162–1174.
13. Fujimoto, H., N. Onishi, N. Kato, M. Takekawa, X.Z. Xu, A. Kosugi, T. Kondo, I. Oishi, A. Yoda, M. Imamura, and Y. Minami. 2006. Regulation of the anti-oncogenic Chk2 kinase by the oncogenic Wip1 phosphatase. *Cell Death Differ*. 13:1170–1180.
14. Kozlov, S., N. Gueven, K. Keating, J. Ramsay, and M.F. Lavin. 2003. ATP activates ataxia-telangiectasia mutated (ATM) in vitro. *J. Biol. Chem*. 278:9309–9317.
15. Kozlov, S.V., M.E. Graham, C. Peng, P. Chen, P.J. Robinson, and M.F. Lavin. 2006. Involvement of novel autophosphorylation sites in ATM activation. *EMBO J*. 25:3504–3514.
16. Pellegrini, M., A. Celeste, S. Difilippantonio, R. Guo, W. Wang, L. Feigenbaum, and A. Nussenzweig. 2006. Autophosphorylation at serine 1987 is dispensable for murine ATM activation in vivo. *Nature*. 443:222–225.
17. Adams, J.M., A.W. Harris, C.A. Pinkert, L.M. Corcoran, W.S. Alexander, S. Cory, R.D. Palmiter, and R.L. Brinster. 1985. The c-myc oncogene driven by immunoglobulin enhancers induces lymphoid malignancy in transgenic mice. *Nature*. 318:533–538.

18. Schmitt, C.A., M.E. McCurrach, E. de Stanchina, R.R. Wallace-Brodeur, and S.W. Lowe. 1999. *INK4a/ARF* mutations accelerate lymphomagenesis and promote chemoresistance by disabling p53. *Genes Dev.* 13:2670–2677.
19. Eischen, C.M., J.D. Weber, M.F. Roussel, C.J. Sherr, and J.L. Cleveland. 1999. Disruption of the ARF-Mdm2-p53 tumor suppressor pathway in Myc-induced lymphomagenesis. *Genes Dev.* 13:2658–2669.
20. Egle, A., A.W. Harris, P. Bouillet, and S. Cory. 2004. Bim is a suppressor of Myc-induced mouse B cell leukemia. *Proc. Natl. Acad. Sci. USA.* 101:6164–6169.
21. Smith, G.C., F. d'Adda di Fagagna, N.D. Lakin, and S.P. Jackson. 1999. Cleavage and inactivation of ATM during apoptosis. *Mol. Cell. Biol.* 19:6076–6084.
22. Hotti, A., K. Järvinen, P. Siivola, and E. Hölttä. 2000. Caspases and mitochondria in c-Myc-induced apoptosis: identification of ATM as a new target of caspases. *Oncogene.* 19:2354–2362.
23. Ramiro, A.R., M. Jankovic, E. Callen, S. Difilippantonio, H.T. Chen, K.M. McBride, T.R. Eisenreich, J. Chen, R.A. Dickins, S.W. Lowe, et al. 2006. Role of genomic instability and p53 in AID-induced c-myc-Igh translocations. *Nature.* 440:105–109.
24. Li, Y., D. Wu, B. Chen, A. Ingram, L. He, L. Liu, D. Zhu, A. Kapoor, and D. Tang. 2004. ATM activity contributes to the tumor-suppressing functions of $p14^{ARF}$. *Oncogene.* 23:7355–7365.
25. Eymin, B., P. Claverie, C. Salon, C. Leduc, E. Col, E. Brambilla, S. Khochbin, and S. Gazzeri. 2006. p14ARF activates a Tip60-dependent and p53-independent ATM/ATR/CHK pathway in response to genotoxic stress. *Mol. Cell. Biol.* 26:4339–4350.
26. Powers, J.T., S. Hong, C.N. Mayhew, P.M. Rogers, E.S. Knudsen, and D.G. Johnson. 2004. E2F1 uses the ATM signaling pathway to induce p53 and Chk2 phosphorylation and apoptosis. *Mol. Cancer Res.* 2:203–214.